

The first 2^+ excited state of ^{24}O

K Tshoo¹, Y Satou¹, T Nakamura², N Aoi³, H C Bhang¹, S Choi¹, S Deguchi², F Delaunay⁴, J Gibelin⁴, T Honda⁵, M Ishihara³, Y Kawada², Y Kondo², T Kobayashi⁶, N Kobayashi², F M Marques⁴, M Matsushita⁵, Y Miyashita⁷, T Motobayashi³, Y Nakayama², N A Orr⁴, H Otsu³, H Sakurai³, S Shimoura⁸, D Sohler⁹, T Sumikama⁷, S Takeuchi³, K N Tanaka², N Tanaka², Y Togano³, K Yoneda³, K Yoshinaga⁷, T Zheng¹⁰, Z H Li³, Z X Cao¹⁰

¹Department of Physics and Astronomy, Seoul National University, Seoul 151-742, Korea.

²Department of Physics, Tokyo Institute of Technology, Tokyo 152-8551, Japan.

³RIKEN Nishina Center, Saitama 351-0198, Japan.

⁴LPC-Caen, ENSICAEN, Université de Caen, CNRS/IN2P3, 14050 Caen cedex, France.

⁵Department of Physics, Rikkyo University, Tokyo 171-8501, Japan.

⁶Department of Physics, Tohoku University, Aoba, Sendai, Miyagi 980-8578, Japan.

⁷Department of Physics, Tokyo University of Science, Noda, Chiba 278-8510, Japan.

⁸Department of Physics, University of Tokyo, Tokyo 113-0033, Japan.

⁹Institute of Nuclear Research of the Hungarian Academy of Sciences, P.O.Box 51, H-4001 Debrecen, Hungary.

¹⁰School of Physics and State Key Laboratory of Nuclear Physics and Technology, Peking University, Beijing 100871, China.

E-mail: tshoo99@snu.ac.kr

Abstract. The unbound excited states of the most neutron-rich dripline oxygen isotope, ^{24}O ($Z=8$, $N=16$), have been investigated using the $^{24}\text{O}(p,p')^{24}\text{O}^*$ reaction at the beam energy of 63 MeV/nucleon in inverse kinematics at RIKEN. The ^{24}O beam was produced in the projectile-like fragmentation process of a 95 MeV/nucleon ^{40}Ar primary beam on the Be production target. The decay energy spectrum of $^{24}\text{O}^*$ in $^{23}\text{O}+n$ channel was reconstructed in the invariant mass of the neutron and the charged fragment detected in coincidence. The first unbound excited state of ^{24}O has been observed at $E_x=4.68^{+0.21}_{-0.14}$ MeV (preliminary) along with the evidence for another higher lying state at around 7.3 MeV. The energy of the former state is compared with existing data and the results of shell-model calculations.

1. Introduction

The change in the magic number and the shell structure observed in neutron rich nuclei is the important factor that characterizes the structure of nuclei close to drip lines. It has been suggested that the new magic number appears at $N=16$ instead of $N=20$ for oxygen isotopes [1]. The excitation energy of the first 2^+ excited state in the even-even nuclei suddenly increases at the magic number, thereby being a strong indicator of the magic number. The first excited state of ^{24}O has been known to lie above the neutron separation energy, which explains the fact that no γ -decay of $^{24}\text{O}^*$ [2] could have been observed so far. Recently, the first 2^+ excited state of ^{24}O was studied by Hoffman et al. in the proton removal reaction of a radioactive ^{26}F

beam [3]. However, the predicted close proximity of the first 2^+ and 1^+ states has hampered the unambiguous interpretation of the data.

Here, we report on the results of the experimental investigation of the first 2^+ excited state of ^{24}O via the $^{24}\text{O}(p,p')^{24}\text{O}^* \rightarrow ^{23}\text{O} + n$ reaction in inverse kinematics at 63 MeV/nucleon performed at RIKEN-RIBF accelerator research facility. While the proton removal reaction on ^{26}F [3] involves complicated reaction processes for the population of the excited states in ^{24}O , much simpler reaction mechanisms are expected for the (p,p') reaction at energies above several tens of MeV.

2. Experiment

The experiment was performed at the RIPS facility [4] operated by the RIKEN Nishina Center. The experimental setup is similar to the preceding measurements [5,6]. A 63 MeV/nucleon secondary beam of ^{24}O was produced in a beryllium production target by the fragmentation of a 95 MeV/nucleon ^{40}Ar primary beam. The secondary beam was selected by magnetic analysis in the fragment separator, RIPS, and the magnetic rigidity was determined from the position measurements in parallel plate avalanche counters (PPAC) mounted at the dispersive focus F1. The momentum acceptance was $\Delta P/P = \pm 3\%$. The time of flight was determined from a time difference between a thin plastic scintillator mounted at the achromatic focus F2 and an RF signal provided by the AVF and Ring cyclotrons. The energy loss of the secondary beam was measured by silicon detector (SSD) of 350 μm mounted at the achromatic focus F2. Particle identification of the secondary beam was performed by the $B\rho$ -TOF- ΔE method. The ^{24}O secondary beam with an intensity of about 4 ions/s was directed towards a liquid-hydrogen reaction target [7] installed at the achromatic focus F3. The target thickness was ~ 160 mg/cm 2 and the midtarget energy of ^{24}O was 63 MeV/nucleon. Background measurements were performed with an empty target cell. A schematic view of the experimental setup is shown in Fig.1.

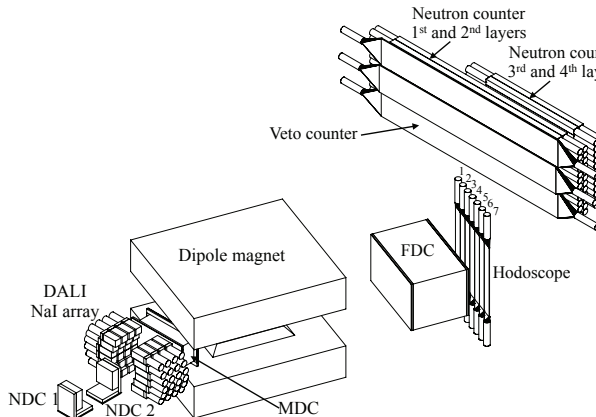


Figure 1. A schematic view of the experimental setup.

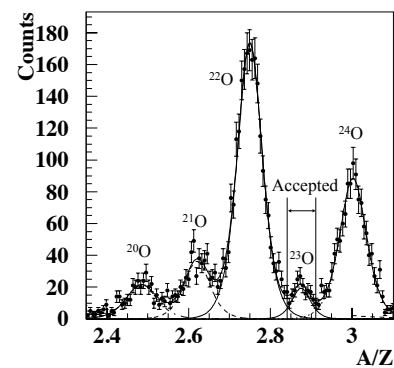


Figure 2. A/Z spectrum for oxygen isotopes.

The trajectory of the secondary beam was determined by tracking using two drift chambers (NDCs) installed in front of the target. The positions and angles on the reaction target were determined by extrapolating the track obtained with NDCs.

The charged fragments emitted from the reaction target were bent by a dipole magnet placed downstream from the target, and their trajectories were measured by two drift chambers, MDC and FDC, placed before and after the dipole magnet, respectively. The angles of fragments

emitted from the target were determined by the hit position difference between the MDC and the target. The time of flight of the fragment was measured between the thin plastic scintillator mounted at the achromatic focus F2 and a hodoscope installed just after the FDC. The flight length from the reaction target to the hodoscope was about 3.57 m. The energy loss of the fragment was also measured in the hodoscope. The magnetic rigidity was determined by measuring the trajectory of the fragment with the dipole magnet. The mass and charge of the fragment were identified by employing the $B\rho$ -TOF- ΔE method. Fig.2 shows the mass spectrum for the oxygen isotopes in coincidence with neutrons.

The neutrons emitted after the decay of $^{24}\text{O}^*$ were detected by a neutron-counter array placed ~ 4.5 m downstream from the target. The neutron counter array covered an angular range $+17^\circ \sim -8^\circ$ in the horizontal and $\pm 4.6^\circ$ in the vertical directions. The total thickness (4 layers) was 24 cm. The effective areas of the neutron counters were $210[\text{W}] \times 74[\text{H}] \text{ cm}^2$ and $106[\text{W}] \times 74[\text{H}] \text{ cm}^2$ for the 1st-2nd and 3rd-4th layers, respectively. All layers were divided into 12 segments of the plastic scintillator bar with 2-inch PMTs at both sides. The momentum vectors of the neutrons were determined from the hit position in the neutron-counter array and the time of flight. The horizontal hit positions were measured from the time difference between the PMTs. The detection efficiencies of the neutron counter were estimated from the $^7\text{Li}(p,n)^7\text{Be}(\text{g.s.}+0.43 \text{ MeV})$ reaction at 70 MeV. To exclude all charged particles emerging from the target, the veto-counters were installed just before the neutron counter.

The decay energy spectrum was reconstructed from the invariant mass of a fragment and a neutron. The decay energy, E_{decay} , is expressed as

$$E_{\text{decay}} = \sqrt{(E_f + E_n)^2 - (\mathbf{P}_f + \mathbf{P}_n)^2} - (M_f + M_n), \quad (1)$$

where $E_f(E_n)$ and $\mathbf{P}_f(\mathbf{P}_n)$ are the total energy and momentum vector of the fragment (neutron), respectively. The $M_f(M_n)$ is the fragment (neutron) mass.

3. Results and discussion

In the ^{24}O nucleus, 8 protons and 16 neutrons are filled up to the $\pi 0p_{1/2}$ orbit and the $\nu 1s_{1/2}$ orbit, respectively. This proton number is a traditional magic number, $Z=8$, which arises from a large single particle energy gap between the $\pi 0p_{1/2}$ orbital and the next $\pi 0d_{5/2}$ orbital. Then, the first excited state of ^{24}O will be attributed to the promotion of a neutron from the $\nu 1s_{1/2}$ orbital to the $\nu 0d_{3/2}$ orbital, and the possible spin-parity values are 1^+ and 2^+ with the configuration of $(\nu 1s_{1/2})^1 \otimes (\nu 0d_{3/2})^1$. The theoretical calculations predict that the excitation energy of the 2^+ state is ~ 1 MeV lower than that of the 1^+ state [8,9,10]. We may expect that the angular momentum of the neutron decaying from the 2^+ state is $l=2$.

A preliminary decay energy spectrum of $^{23}\text{O}+n$ is shown in Fig.3. The error bars are statistical ones. The effects of finite detector acceptances were not corrected. To subtract the contributions originating from the ^{22}O and ^{24}O fragments, the decay energy spectra of $^{22}\text{O}+n$ and $^{24}\text{O}+n$ were normalized by the ratio of the particles measured in the given mass gates, and the decay energy spectra of $^{22}\text{O}+n$ and $^{24}\text{O}+n$ were subtracted from that of $^{23}\text{O}+n$. The simulated decay energy spectrum including the experimental resolutions and acceptances was compared with experimental data in order to extract the resonance energy. In the simulation, the energy dependent single Breit-Wigner line shape assuming the d -wave neutron was used to generate the resonance shape, where the level width $\Gamma_l(E_{\text{decay}})$ was calculated from the penetrability P_l in ref. [11]:

$$\sigma_l(E_{\text{decay}}) \sim \frac{\Gamma_r \Gamma_l(E_{\text{decay}})}{(E_{\text{decay}} - E_r)^2 + \Gamma_l^2(E_{\text{decay}})/4}, \quad (2)$$

$$\Gamma_l(E_{\text{decay}}) = \Gamma_r P_l(E_{\text{decay}})/P_l(E_r), \quad (3)$$

By minimizing the χ^2 , the resonance energy of the first unbound state of ^{24}O was determined to be 590^{+160}_{-60} keV. This preliminary result is consistent with the previous study[3]. A new state was observed at $E_{\text{decay}} \sim 3.2$ MeV, but the nature of this state has yet been unidentified in the present analysis. The excitation energy E_x of the first excited state was calculated to be $4.68^{+0.21}_{-0.14}$ MeV from the relation $E_x = E_r + S_n$ by adopting the one-neutron separation energy of $S_n = 4.09 \pm 0.13$ MeV taken from ref. [12].

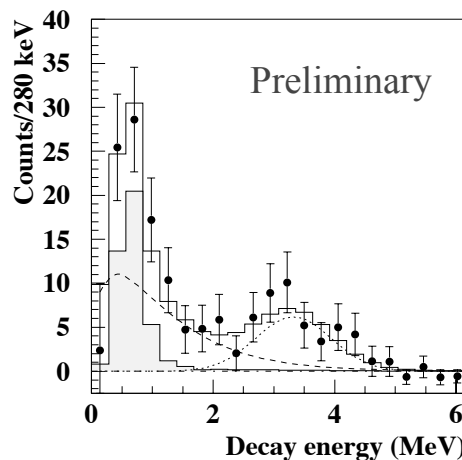


Figure 3. Preliminary decay energy spectrum of $^{23}\text{O}+n$. The shaded histogram corresponds to the simulated resonance contribution with the energy dependence Breit-Wigner line shape assuming the d -wave neutron. The dashed line is nonresonant contribution. The second peak (dotted line) was assumed to be a Gaussian shape. The solid histogram corresponds to the sum of dashed, dotted lines and shaded histogram.

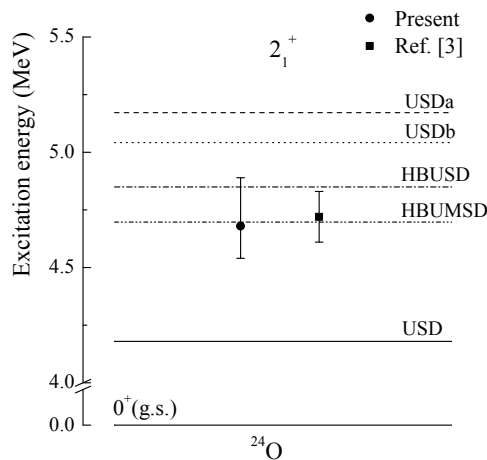


Figure 4. The excitation energy of the first 2^+ state measured in the present experiment (filled circle) as compared to that of ref. [3] (filled square). Results of shell-model calculations [8,9,10] are also shown.

Fig.4 shows the comparison of the observed excitation energy of the first 2^+ state with that of ref. [3], and with those of calculated shell model [8,9,10]. The calculations were carried out in the sd model space using the code Nushell@MSU [13]. The prediction using the standard shell-model interaction (USD) [8] underestimates the excitation energy of the 2_1^+ state, and its newer versions USDa and USDb [9] overestimate the energy. The HBUSD and HBUMSD interactions [10], which are the modified versions of the USD, reproduce the experimental results more successfully, in particular the HBUMSD.

4. Summary

We have investigated the unbound excited state of ^{24}O using the invariant mass method in the $^{23}\text{O}+n$ decay channel via the proton inelastic scattering of ^{24}O in inverse kinematics. The first excited state of ^{24}O has been observed at the decay energy of $E_{\text{decay}}=590_{-60}^{+160}$ keV (preliminary) along with the evidence for another higher excited state at $E_{\text{decay}}\sim 3.2$ MeV. The corresponding excitation energy of the first excited state is $4.68_{-0.14}^{+0.21}$ MeV.

Acknowledgments

We would like to thank the accelerator staff of RIKEN for their excellent operation. This work is supported by the Grant-in-Aid for Scientific Research (No. 19740133) from MEXT Japan and WCU program of NRF (Grant No. R32-2008-000-10155-0) and KOSEF(Grant No. R01-2007-000-11714-0) of Korea.

References

- [1] A. Ozawa, et al., Phys. Rev. Lett. **37**, 5493 (2000).
- [2] M. Stanoiu, et al., Phys. Rev. C **69**, 034312 (2004).
- [3] C. R. Hoffman, et al., Phys. Lett. B **672**, 17 (2009).
- [4] T. Kubo, et al., Nucl. Instrum. Methods Phys. Res. B **70**, 309 (1992).
- [5] Y. Kondo, et al., Phys. Lett. B **690**, 245 (2010).
- [6] Y. Satou, et al., Phys. Lett. B **660**, 320 (2008).
- [7] H. Ryuto, et al., Nucl. Instrum. Methods Phys. Res. A **555**, 1 (2005).
- [8] B. Brown and B. Wildenthal, Annu. Rev. Nucl. Part. Sci. **38**, 29 (1988).
- [9] B. A. Brown and W. A. Richter, Phys. Rev. C **74**, 034315 (2006).
- [10] B. Brown, W. Richter, R. Julies, and B. Wildenthal, Ann. Phys. (N.Y.) **182**, 191 (1988).
- [11] A. M. Lane and R. G. Thomas, Rev. Mod. Phys. **30**, 257 (1958).
- [12] B. Jurado, et al., Phys. Lett. B **649**, 43 (2007).
- [13] Nushell@MSU, B. A. Brown and W. D. M. Rae, MSU-NSCL report (2007).